Studies of {[1](1,1′)Ferroceno[1](1,1′)ruthenocenophane}-1-ylium Hexafluorophosphate and Related α-Carbonium Salts

Masanobu Watanabe,* Izumi Motoyama, and Toshio Takayama

Department of Chemistry, Faculty of Engineering, Kanagawa University, Rokkakubashi, Yokohama 221

(Received April 30, 1996)

The oxidation of [1](1,1′)ferroceno[1](1,1′)ruthenocenophane ([1.1]FcRc) and ferrocenylruthenocenylmethane ($FcCH_2Rc$) with bromo- or chlorobis(η^5-cyclopentadienyl)ruthenocenium(1+) hexafluorophosphates gave the title compound, $[Fe(C_5H_4CH_2C_5H_4)(C_5H_4CH^+C_5H_4)Ru]PF_6^-$ (**1**), as an α-carbonium salt and ferrocenylruthenocenylmethylium$^+$ hexafluorophosphate $[FeCp(C_5H_4CH^+C_5H_4)CpRu]PF_6^-$ (**3**), respectively. The crystal of **1** has been found to be triclinic, space group $P\bar{1}$, $a = 10.572(9)$, $b = 10.581(3)$, $c = 9.680(5)$ Å, $\alpha = 99.50(3)°$, $\beta = 108.14(5)°$, $\gamma = 88.30(5)°$, $Z = 2$, and the final $R = 0.082$ and $R_w = 0.094$. The distance between the Ru and Fe is 4.507(3) Å; which is much shorter than the value of neutral [1.1]FcRc one (4.792(2) Å). The two C_5H_4-rings in the Rc moiety are tilted largely (the tilting angle is 10.74°) due to a strong Ru···C_α (α-metylium) interaction. The crystal of **3** has been found to be orthorhombic, space group P_{bca}, $a = 17.062(5)$, $b = 19.172(6)$, $c = 12.580(7)$Å, $Z = 8$, and the final $R = 0.067$ and $R_w = 0.072$. The tilting angle of the Rc moiety is 7.98°. The most interesting difference between **1** and **3** is found in the distance between the Ru and C_α atoms; i.e., the distance of **3** (2.43(2) Å, closer to the Ru–C covalent bond) is significantly shorter than the value of **1** (2.51(1) Å, somewhat longer to the covalent bond); therefore, the greater positive $-CH^+-$ charge can be stabilized by a delocalization of the charge over the $[RuCp(C_5H_4CH)]^+$ fragment for **3**. However, the $-CH^+-$ charge is spread out over $[Fe(C_5H_4CHC_5H_4)(C_5H_4CH_2C_5H_4)Ru]^+$ for **1**. Temperature-dependent ^{57}Fe-Mössbauer spectroscopy (areal intensity ratio of ferrocene and ferrocenium) supports above the conclusion.

The chemistry of [1.1]metallocenophanes has been investigate from the several points of view by Westerhoff et al.[1—6] [1](1,1′)-Ferroceno[1](1,1′)ruthenocenophane ([1.1]-FcRc) is one of the interesting [1.1]metallocenophanes because the Rc and Fc moieties exist in a syn form; thus, some interaction between them may be expected, like in the case of [1.1]ruthenocenophane dication.[6] Recently, the oxidation of [1.1]FcRc with halobis(η^5-cyclopentadienyl)-ruthenocenium$^+$ tetrafluoroborate ($[(RcH)X]^+BF_4^-$, X = Cl, Br) was carried out by the present authors, and the oxidation product was found to have an α-carbonium structure (**2**), formulated as $[Fe^{II}(C_5H_4CH_2C_5H_4)(C_5H_4CH^+C_5H_4)-Ru^{II}]$ based on the results of the X-ray diffraction and ^{13}C CP/MAS NMR spectroscopic studies, as shown in Scheme 1 and Fig. 1.[7] Although the $Ru^{II}\cdots Fe^{II}$ distance (4.495(2) Å) is ca. 0.3 Å smaller than the value of the neutral one, which shows no interaction between them. The most interesting structural feature is found in the formation of the Ru–CH^+ covalent bond (2.407(6) Å), which gives the stability of the higher positive carbonium CH^+ charge. ^{57}Fe-Mössbauer and ^{13}C CP/MAS NMR studies support this conclusion. To extend our studies, an analogous hexafluorophosphate **1** was prepared. The result of ^{13}C CP/MAS NMR and ^{57}Fe-Mössbauer studies of **1** are quite different from those of the reported analogous tetrafluoroborate **2** and hexafluorophosphate **3**;[7,8] i.e., although several sharp ^{13}C CP/MAS NMR peaks are observed for **2**, no clear NMR peaks are observed for **1**. Moreover, **2** and **3** give ferrocene-like ^{57}Fe-Mössbauer spectra over all temperatures; **1** gives ferrocene and ferrocenium-like spectra with temperature-dependent areal intensity ratio. Therefore, some interactions may be expected between the Fe and the remaining fragment ($(C_5H_4CH^+C_5H_4)Ru^{II}$). The aim of the present studies was to investigate the crystal structures of **1** and **3** in comparison with that of the reported **2**, and to verify the different results of their ^{57}Fe-Mössbauer and ^{13}C CP/MAS NMR spectroscopies from a structural point of view.

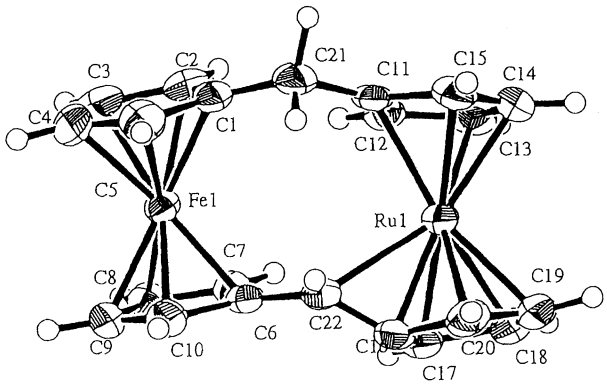

Fig. 1. ORTEP drawing of cation **2**.

Experimental

Syntheses. Hexafluorophosphate **1** was prepared by the same methods of **2** by using $[(RcH)X]^+PF_6^-$ instead of $[(RcH)-X]^+BF_4^-$ (X=Cl or Br).[7] Found: C, 45.31; H, 3.31%. Calcd for

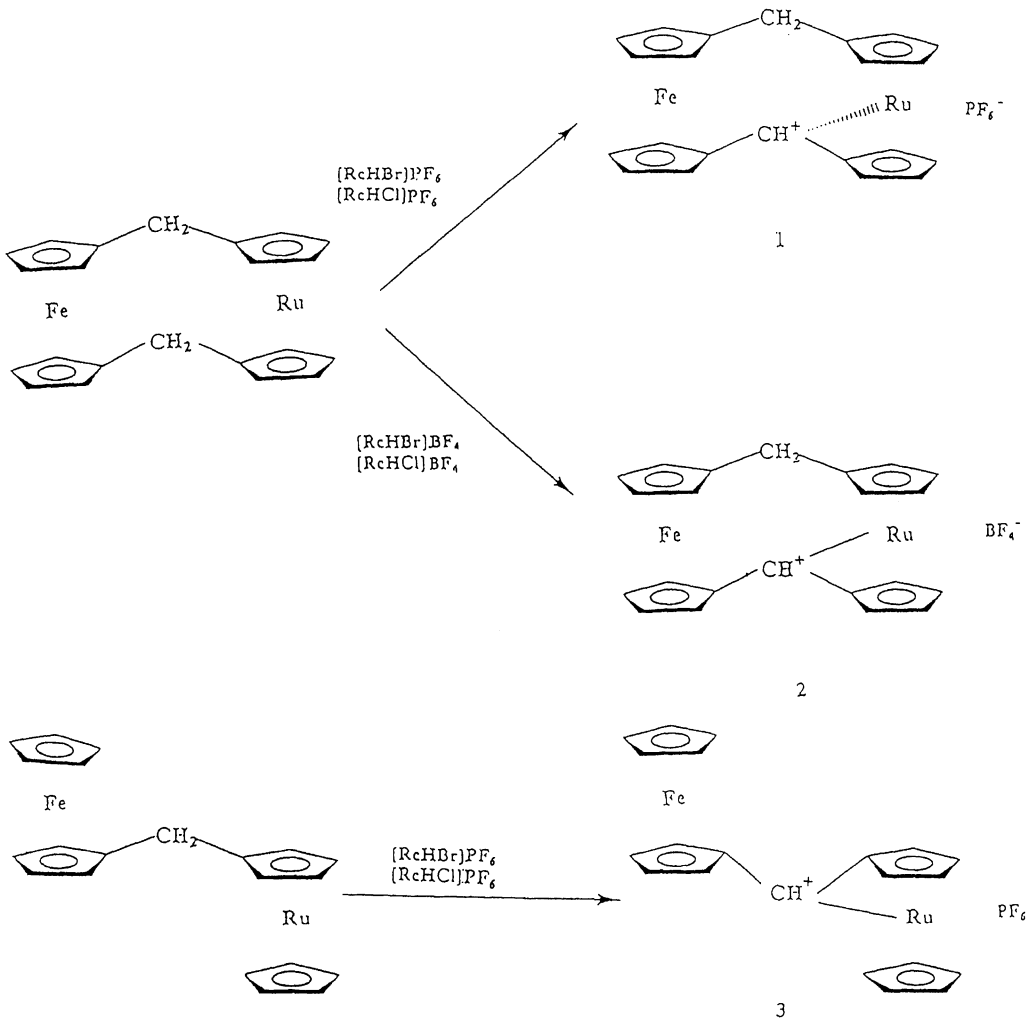

Scheme 1.

$C_{22}H_{19}PF_6FeRu$: C, 45.14; H. 3.27%. Hexafluorophosphate **3** was prepared by the same method reported previously.[8] Single crystals of **1** and **3** suitable for X-ray studies were obtained by the diffusion of hexane vapor into a CH_2Cl_2 solution of **1** and **3** at ca. 260 K.

^{57}Fe-Mössbauer and NMR Measurements. ^{57}Fe-Mössbauer measurements were carried out using a ^{57}Co(Rh) source moving in a constant acceleration mode. The isomer-shift (IS) value was referred to metallic foil, and the experimental error of the IS and quadrupole splitting (QS) values was 0.02 mm s^{-1}. The Mössbauer parameters were obtained by a least-squares fitting to a Lorentzian peak. The ^{1}H (500.16 MHz) and ^{13}C CP/MAS NMR spectra were recorded under the same conditions as previously reported.[8]

X-Ray Structural Analysis. Crystals of **1** (0.2×0.3×0.2 mm) and of **3** (0.3×0.1×0.03 mm) were selected. X-Ray diffraction experiments were carried out on a Rigaku AFC-6A automated four-circle X-ray diffractometer with graphite monochromatized Mo $K\alpha$ radiation ($\lambda = 0.71073$ Å). The intensity data were collected at 25±1° using the ω–2θ scan mode with a scanning speed of 4° min^{-1}. The cell constants and an oriental matrix for the data collection were obtained from a least-squares refinement using 25 reflections in the range $22 < 2\theta < 25°$. The crystal stability was checked by recording three standard reflections every 150 reflection; no significant variations were observed. The structures of **1** and **3** were solved by heavy-atom Patterson methods and expanded using Fourier techniques.

For **1**, of the 6219 reflections collected in the range $4° \leqq 2\theta \leqq 60°$, 5918 were unique ($R_{int} = 0.024$), of which 3578 reflections with $I_{obsd} > 2\sigma$ (I_{obsd}) were used for a structure determination. The scan width was $1.68 + 0.3 \tan\theta$. The 154 refinement variable parameters converged to $R = \sum||F_o| - |F_c||/\sum|F_o| = 0.082$, $R_w = [\sum w(|F_o| - |F_c|)^2/\sum wF_o^2]^{1/2} = 0.094$, and the standard deviation of the observation of unit weight (s) was 2.67. For **3**, 2844 reflections were collected in the range $4° < 2\theta < 50°$, of which 1165 reflections with $I_{obsd} > 2\sigma(I_{obsd})$ were used for a structure determination. The scan width was $0.89 + 0.3 \tan\theta$. The 256 refinement variable parameters converged to $R = 0.067$, $R_w = 0.072$, and $s = 1.98$.

The non-hydrogen atoms were refined anisotropically by a full-matrix least-squares calculation. The hydrogen atoms of CH^+ and methylene were located based on difference Fourier maps; the other hydrogen atoms were fixed at the calculated positions, and were refined isotropically. The neutral-atom scattering factors were taken from Cromer and Waber;[9] anomalous dispersion-effect corrections were included in F cal,[10] in which the values for $\Delta f'$ and $\Delta f''$ were those of Creagh and McAuley.[11] All of the calculations were performed using the TEXSAN crystallographic software package.[12] The complete $F_o - F_c$ data are deposited as Document No. 69056 at the Office of the Editor of Bull. Chem. Soc. Jpn.

Results and Discussion

Crystal Structure of Hexafluorophosphate 1. The results of ^{57}Fe-Mössbauer spectroscopies of **1** compared with studies of **2** and **3** are discussed first. The latter two salts gave the ferrocene-like Mössbauer spectra over all the temperatures, as previously reported; i.e., the QS and IS values of **2** and **3** at 78 K were reported to be 1.89, 0.50 mm s^{-1} and 2.24 and 0.52 mm s^{-1}, respectively.[7,8] Both QS values are much smaller than the values of the corresponding neutral one (ca. 2.4 mm s^{-1}) and closer to some reported analogous α-carbonium cations, such as FcCH$^+$ Fc (ca. QS 2.1 mm s^{-1}) and [Fe($C_5H_4CH^+C_5H_4$)($C_5H_4CH_2C_5H_4$)Fe] (QS; 1.80 mm s^{-1}).[3—5,13,14] Mueller–Westerhoff explained the latter small QS value (1.80 mm s^{-1}) as follows: The positive CH$^+$ fragment may be pulled to the central Fe atoms so as to allow a direct Fe–CH$^+$ interaction, resulting in a positive charge delocalization over the Fc moiety (both Fe atoms have 1/3 positive charge), which gives the smaller QS value observed for the cations. However, the distances of Fe–CH$^+$ are 2.96 and 3.01 Å; these values are too long to estimate for the covalent Fe–C$^+$ (σ) (ca. 2.1 Å). It is already established that the α-carbonium cations have a fulvene-type character, in which there is a double-bond character between the C$^+$ and the neighboring C_5H_4 ring carbon (C_1, C^+=C_1). Therefore, the smaller QS value may be caused by a strong interaction between the Fe and the double bond, such as the donation of d-electrons (e_{2g}) of Fe to the empty π^*-orbital. Since a similar smaller QS value is found for **2**, the same interaction is expected for **2**. Unlike in the cases of **2** and **3**, **1** gave a large temperature-dependent Mössbauer spectra. The Mössbauer spectra and its parameters are given in Fig. 2 and Table 1. Two kinds of Fe atoms (typical ferrocenium-type (QS; 0.40 and IS; 0.51 mm s^{-1}) and ferrocene-type (QS; 2.21 and IS; 0.52 mm s^{-1}) were observed at 78 K. The ferrocenium-type areal intensity ratio ($\varkappa$ = Fe(III)/Fe(II) + Fe(III)) has been estimated to be 0.52. With increasing temperature, an increasing ferrocenium-type species is observed (the $\varkappa$ is estimated to be 0.80 at 300 K). These temperature dependences of the areal intensity ratio are much larger than those found in a number of mixed-valence (trapped-valence type) biferrocene derivatives; thus, these spectral features cannot be ascribed to only the recoil-free fractional difference between the Fe^{II} and Fe^{III}, but to some interaction between the Fe and the [Ru($C_5H_4CH^+$)] fragment.

A similar spectral difference between **1** and **2** has been observed for the ^{13}C CP/MAS NMR spectra at room temperature. Although some sharp NMR signals has been observed for the reported **2**,[7] much broader NMR signals were observed for **1** (no δ values are given) due to the paramagnetic species. All of the results clearly suggest that the oxidation state of the Fe atom in **1** is much higher than compared with that of the neutral [1.1]FcRc and analogous salts, **2** and **3** (Fe^{II}).

To verify the these spectral differences between **1** and **2**, an X-ray diffraction study of **1** was carried out. The crystallographic data and some of the experimental conditions

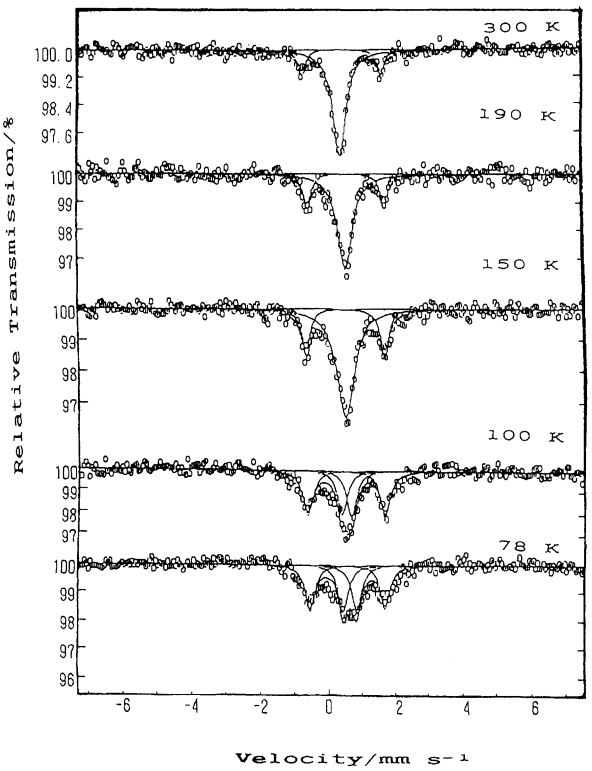

Fig. 2. ^{57}Fe-Mössbauer spectra of **1** at indicated temperatures.

Table 1. ^{57}Fe-Mössbauer Parameters of **1**—**3**

Compounds	T/K	QS/mm s^{-1}	IS/mm s^{-1}	$\varkappa$[a]
1	300	2.32	0.48	
		0.0	0.42	0.80
	190	2.27	0.52	
		0.0	0.52	0.73
	150	2.25	0.51	
		0.0	0.49	0.71
	100	2.23	0.51	
		0.32	0.50	0.55
	78	2.21	0.52	
		0.40	0.51	0.52
2	300	1.86	0.42	
	200	1.91	0.45	
	78	1.89	0.50	
3	300	2.19	0.43	
	78	2.24	0.52	

a) Areal intensity ratio of ferrocenium species (Fe(III)/Fe(II)+Fe(III)).

for the X-ray structure analysis are listed in Table 2; also, the final atomic coordinates and equivalent isotropic temperature factors (B_{eq}) of non-hydrogen atoms, selected bond distances, and dihedral angles are given in Tables 3, 4, and 5, and ORTEP drawings of the cation are shown in Fig. 3 along with the atom numbering.

As shown in Fig. 3, the cation keeps in *syn*-conformation, as does **2**. The Fe···Ru distance (4.507(3) Å), which is much shorter than the value (4.792(2) Å[15]) of neutral one and closer to the value of **2** (4.495(2) Å[7]) suggests no metal–metal in-

Table 2. Crystal and Intensity Collection Data for **1**, **3**

Compound	**1**	**3**
Formula	$C_{22}H_{19}FeRuPF_6$	$C_{21}H_{19}FeRuPF_6$
Formula weight	586.28	573.26
Space group	*P*1	*Pbca*
a/Å	10.572(9)	17.062(5)
b/Å	10.581(3)	19.172(6)
c/Å	9.680(5)	12.580(7)
α/°	99.50(3)	—
β/°	108.14(5)	—
γ/°	88.30(5)	—
V/Å^3	1014.5(10)	4116(5)
Z	2	8
D_X/cm^{-3}	1.919	1.850
T/°C	23	23
λ/Å	0.71073	0.71073
μ/cm^{-1}	15.99	15.74
No. of ref.	5918	2844
No. of obsd	3578 ($I > 2\sigma(I)$)	1165 ($I > 2\sigma(I)$)
R	0.082	0.067
R_W	0.094	0.072

teraction. The two C_5H_4 rings of the Rc and Fc moieties differ from eclipsed, and the rotation angles of Fc and Rc are 12(1) and 14(2)°, respectively. The two C_5H_4 rings of the Rc moiety are greatly tilted; the tilting angles of the Rc and Fc moieties are 10.74° and 5.16°, respectively, the former is closer to the value of **2** (10.92°). Based on the results of difference Fourier maps, C(21) and C(22) have a methylene and methine character, respectively; thus, the cation **1** may be considered to be an α-carbonium cation analogous

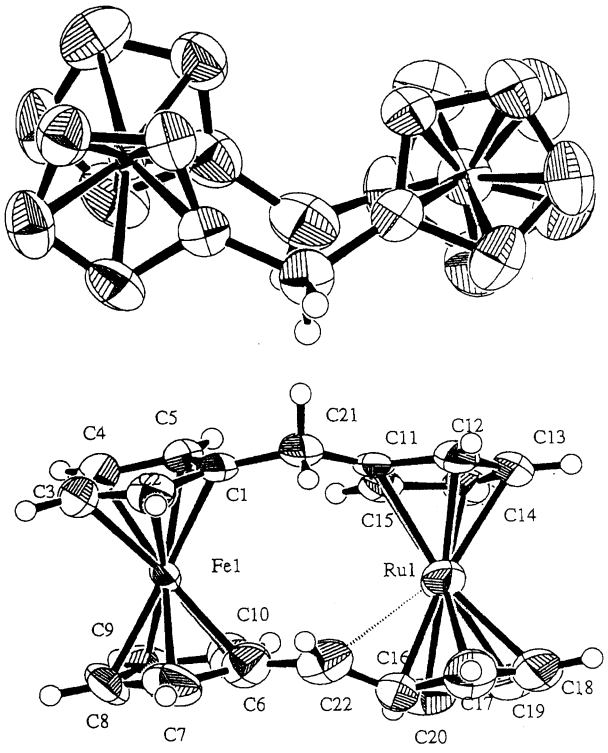

Fig. 3. ORTEP drawing of cation **1** showing the crystallographic numbering.

Table 3. Atomic Coordinates and Isotropic Temperature Factors (Å^2) for **1**

Atom	x	y	z	B_{eq}[a)]/Å^2
Ru(1)	0.2607(1)	0.1246(1)	−0.1547(1)	4.2
Fe(1)	0.2648(1)	0.4179(1)	−0.4423(1)	2.5
P(1)	0.7829(4)	0.2436(4)	0.8429(5)	5.9
F(1)	0.881(1)	0.278(1)	0.771(2)	15.2
F(2)	0.677(2)	0.187(2)	0.715(2)	28.1
F(3)	0.702(1)	0.215(1)	0.941(2)	16.5
F(4)	0.891(2)	0.269(3)	0.977(2)	26.1
F(5)	0.708(1)	0.363(1)	0.826(2)	15.3
F(6)	0.841(1)	0.106(1)	0.836(2)	14.5
C(1)	0.294(1)	0.223(1)	−0.538(1)	3.3
C(2)	0.389(1)	0.318(1)	−0.549(1)	4.4
C(3)	0.319(1)	0.411(1)	−0.631(1)	5.1
C(4)	0.184(1)	0.382(1)	−0.668(1)	4.9
C(5)	0.170(1)	0.271(1)	−0.612(1)	3.9
C(6)	0.311(1)	0.431(1)	−0.224(1)	5.1
C(7)	0.382(1)	0.523(1)	−0.257(2)	6.1
C(8)	0.295(2)	0.604(1)	−0.340(2)	5.9
C(9)	0.162(1)	0.559(1)	−0.353(1)	5.7
C(10)	0.179(1)	0.457(1)	−0.277(1)	5.1
C(11)	0.252(1)	0.064(1)	−0.390(1)	3.2
C(12)	0.293(1)	−0.041(1)	−0.310(1)	4.6
C(13)	0.188(1)	−0.070(1)	−0.255(1)	5.1
C(14)	0.086(1)	0.017(1)	−0.295(1)	4.3
C(15)	0.126(1)	0.101(1)	−0.375(1)	3.4
C(16)	0.353(1)	0.293(1)	−0.023(1)	5.1
C(17)	0.429(1)	0.182(1)	0.039(1)	6.0
C(18)	0.338(2)	0.118(1)	0.084(1)	5.9
C(19)	0.211(2)	0.180(1)	0.051(1)	6.6
C(20)	0.220(1)	0.289(1)	−0.011(1)	5.6
C(21)	0.334(1)	0.112(1)	−0.471(1)	4.1
C(22)	0.383(1)	0.330(1)	−0.135(1)	5.5
H(21a)	0.317(9)	0.043(8)	−0.564(10)	4.8
H(21b)	0.430(9)	0.103(8)	−0.410(10)	4.8
H(22)	0.466(10)	0.343(9)	−0.138(11)	5.8

a) $B_{eq} = 4/3(B_{11}a^2 + B_{22}b^2 + B_{33}c^2 + B_{13}ac\cos\beta)$. B_{ij}'s are defined by $\exp[-(h^2B_{11} + k^2B_{22} + l^2B_{33} + 2klB_{23} + 2hlB_{13} + 2hkB_{12})]$.

to **2**. However, it is necessary to consider the structure of **1** compared with that of **2** in detail in order to verify the difference in their Mössbauer studies. The Ru–Cp and Ru–C_{ring} distances are 1.792(9) and 2.17(4) Å, respectively, which are somewhat shorter than the corresponding values of **2** (1.801(4) and 2.18(4) Å). While the Fe–Cp (1.668(9) Å) and Fe–C_{ring} (2.06(3) Å) distances are significantly longer than the values of **2** (1.643(4) and 2.04(1) Å, respectively), the Fe–C_{ring} value is the mean value of the ferrocenium cation (2.075 Å[16]) and ferrocene (2.045 Å[17]). This result corresponds well to those of the Mössbauer and CP/MAS NMR spectroscopies; i.e., the oxidation state of Fe in **1** is closer to the ferrocenium character. It can thus be concluded that the positive CH^+ charge is spread out to not only the Rc moiety but also to the Fc moiety giving a ferrocenium species for **1**, unlike in the case of **2**.

These difference between **1** and **2** may be caused by the distance between the Ru and carbonium center (CH^+); i.e., the distance of **1** has been found to be 2.51(1) Å. which

Table 4. Selected Interatomic Distances for **1**

Atom 1–Atom 2	Dist./Å	Atom 1–Atom 2	Dist./Å
Ru–Fe	4.507(3)	Ru–C(22)	2.51(1)
Fe–C(1)	2.11(1)	Fe–C(2)	2.07(1)
Fe–C(3)	2.07(1)	Fe–C(4)	2.06(1)
Fe–C(5)	2.09(1)	Fe–C(6)	2.00(1)
Fe–C(7)	2.01(1)	Fe–C(8)	2.04(1)
Fe–C(9)	2.05(1)	Fe–C(10)	2.05(1)
Ru–C(11)	2.23(1)	Ru–C(12)	2.21(1)
Ru–C(13)	2.18(1)	Ru–C(14)	2.15(1)
Ru–C(15)	2.14(1)	Ru–C(16)	2.08(1)
Ru–C(17)	2.16(1)	Ru–C(18)	2.21(1)
Ru–C(19)	2.20(1)	Ru–C(20)	2.16(1)
C(1)–C(2)	1.43(1)	C(1)–C(5)	1.38(1)
C(2)–C(3)	1.41(1)	C(3)–C(4)	1.39(1)
C(4)–C(5)	1.41(1)	C(6)–C(7)	1.39(2)
C(6)–C(10)	1.36(2)	C(7)–C(8)	1.39(2)
C(8)–C(9)	1.45(2)	C(9)–C(10)	1.38(2)
C(11)–C(12)	1.43(1)	C(11)–C(15)	1.42(1)
C(12)–C(13)	1.44(2)	C(13)–C(14)	1.40(2)
C(14)–C(15)	1.42(1)	C(16)–C(17)	1.50(2)
C(16)–C(20)	1.45(2)	C(17)–C(18)	1.40(2)
C(18)–C(19)	1.45(2)	C(19)–C(20)	1.40(2)
C(1)–C(21)	1.49(1)	C(11)–C(21)	1.49(1)
C(6)–C(22)	1.52(2)	C(16)–C(22)	1.33(2)
P–F(1)	1.50(1)	P–F(2)	1.44(1)
P–F(3)	1.53(1)	P–F(4)	1.43(2)
P–F(5)	1.48(1)	P–F(6)	1.56(1)

Table 5. Selected Bond Lengths (Å) of **1**—**3** and Angle (deg)

	1	**2**	**3**
Fe···Ru	4.507(3)	4.495(2)	5.296(4)
Fe–Cp[a)]	1.668(9)	1.643(4)	1.647(3)
Ru–Cp[b)]	1.792(9)	1.801(4)	1.815(9)
Fe–C_{ring}(av)	2.06(3)	2.04(1)	2.01(4)
Ru–C_{ring}(av)	2.17(4)	2.18(4)	2.16(4)
C_{ring}–C_{ring}(Fe)	1.40(6)	1.42(1)	1.41(4)
C_{ring}–C_{ring}(Ru)	1.37(9)	1.42(3)	1.42(5)
Fe···CH^+	3.13(1)	3.208(6)	3.02(2)
Ru···CH^+	2.51(1)	2.407(6)	2.43(2)

a) Fe–Cp; the mean distance between the Fe and η^5-Cp and η^5-C_5H_4 rings. b) Ru–Cp; the mean distance between the Ru and η^5-Cp and η^5-C_5H_4 rings.

Dihedral Angles between Planes (deg) for **1**

Plane	C(6)–C(10)	C(11)–C(15)	C(16)–C(20)
C(1—5)	5.16	17.17	24.52
C(6—10)	—	20.72	29.10
C(11—15)	—	—	10.74

Dihedral Angles between Planes (deg) for **3**

Plane	C(6)–C(10)	plane C(11)–C(15)	C(16)–C(20)
C(1)–C(5)	2.20	50.27	42.47
C(6)–C(10)	—	50.08	42.20
C(11)–C(15)	—	—	7.98

is somewhat longer than the covalent Ru–C bond (0.25 Å longer than the sum of covalent radii of C(0.77 Å)[18] and Ru (1.48 Å)[19]) and that of **2** (2.407(6) Å),[7] as shown in Table 5. Because of the significantly longer Ru–C_α distance of **1**, the positive CH^+ charge may be stabilized by a delocalization of its charge to all of the moieties. Actually, the Fe···C^+ (22) distance (3.13(1) Å) is somewhat smaller than the value of **2** (3.16(1) Å).

The longer C(22)···Ru distance compared with the value of **2** gives a smaller inclination angle (β; 29.90°) of the C(16)–C(22) bond to the plane C(16—20) compared with the value of **2** (35.1°). The good planarity of the C_5H_4 plane C(16—20) is explained by the same reason; i.e, the bending angle (α) between the C(17—20) plane and the C(20–16–17) plane is 0.69°, which is much smaller than the value of **2** (2.95°).

It is useful to discuss the difference between **1** and **2** from the point of packing. A projection of the unit cell of **1** along the *b* axis is shown in Fig. 4. The octahedral PF_6^- shows a larger thermal motion (B_{eq}; 14.5—28.1 Å^2), as in the case of other PF_6^- salts. The average P–F distance is 1.49(5) Å. The shortest distance between each F and C atoms in the cation are within the range of 3.24—3.56 Å, and the values suggest no van der Waals contact between them. The shortest distance between H(22) and F is found to be 2.71(9) Å (F(5)···H-(22)), implying that no interaction exists between the PF_6^- and α -carbonium –CH^+–. However, **2** gives a much shorter distance between H(22) and one of the F in BF_4^- (2.40 Å, which is shorter than the sum of van de Waals radii of H and F), implying the presence of a hydrogen bond between the CH^+ and BF_4^- anion for **2**, as described in our studies.[7] Because of the smaller ionic radii of BF_4^- compared with that of PF_6^-, BF_4^- can sit closer to the higher positive α-carbonium center, resulting in the formation of a hydrogen bond between them; i.e., the hydrogen bond gives stability to the α-carbonium center for **2**. Due to absence of a hydrogen bond between the PF_6^- and CH^+, the carbonium ion may be stabilized by a delocalization of its positive charge over the

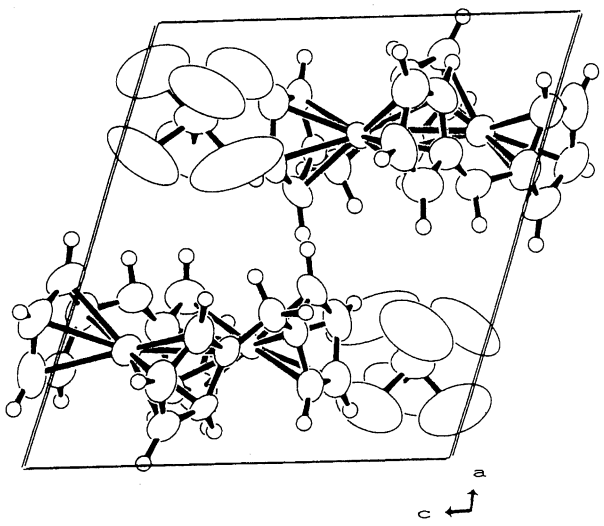

Fig. 4. Packing plot projected along *b* for **1**.

Rc and Fc moieties at lower temperatures. Because of the lower oxidation potential of the Fe than the Ru, the positive charge is located in the Fc moiety and thus ferrocenium-type ^{57}Fe-Mössbauer spectra are observed mainly at room temperature.

Crystal Structure of Hexafluorophosphate 3. To verify the different points of Mössbauer studies between **1** and **3** containing the same PF_6^-, an X-ray diffraction study of **3** was carried out. The salt **3** crystallized on the orthorhombic space group P_{bca}. The final atomic coordinates and equivalent isotropic temperature factors of the non-hydrogen atoms and select interatomic distance are given in Tables 6 and 7; also ORTEP drawing of the cations **3** are shown in Fig. 5 along with the atom numbering. As shown in Fig. 5, the Fc and Rc moieties are in a transoid conformation, as in the case of the analogous diferrocenylmethylium cation, formulated as $[Fe^{II}Cp(C_5H_4CH^+C_5H_4)CpFe^{II}]$.[20] A much longer Fe and Ru distance (5.296(4) Å) is observed compared with the values of **1** and **2**, due to the transoid conformation. The mean Fe–C_{ring}, Fe–Cp, Ru–C_{ring}, and Ru–Cp distances are found to be 2.01(4), 1.647(3), 2.16(4), and 1.815(9) Å, respectively, and all of the values correspond well those of **2**; thus, the oxidation state of Fe must be Fe^{II}. Moreover, the result of difference Fourier maps show that C(21) has a methine character; thus, the cation is formulated as α-carbonium $[\{Fe^{II}Cp(C_5H_4)\}–CH^+–\{Ru^{II}Cp(C_5H_4)\}]$. As in the case of salts **1** and **2**, the Cp and C_5H_4-rings of the Ru side in **3** are greatly tilted; the tilting angle is 7.98°. Unlike in the case of **1**, the Cp and C_5H_4-rings of the Fc and Rc moieties are nearly staggered; the rotation angle of the Fe and Ru moieties are found to be 38(3)° and 34(2)°, respectively.

The most interesting point concerning structure **3** is found in the distance between the Ru and $C^+(21)$; i.e, the distance (2.43(2) Å) is closer to the value of **2** (2.407(6) Å) and shorter than that of **1** (2.51(1) Å); this implies the formation of a Ru–CH^+ covalent bond. Thus, the greater positive CH^+ charge can be spread out within the range of the $[RuCpC_5H_4CH]^+$ fragment only, and the formal oxidation state of Fe in Fc moiety is Fe^{II}. Therefore, **3** gives a temperature-independent ferrocene-like ^{57}Fe-Mössbauer spectra, as with **2**.

The shortest distance between the H(21) and one of the F in PF_6^- (2.69(5) Å; F(2)···H(21)), which is much longer than that of **2** (2.40(4) Å[7]), indicates no hydrogen bond between them, as in the case of **1**. The biggest structural difference of **3** compared with those of **1** and **2** is found in the large inclination angle (β=37.80°, which is larger than the values of rigid structure of **1** (29.90°) and **2** (35.1°)) suggesting a stable Ru–CH^+ in **3**. It has been reported that the large inclined CH^+ bond to the C_5H_4-ring gives stability of the α-carbonium cation; e.g., much large β values (40.3 and 41.8°) are reported for analogous $[C_5(CH_3)_5M(CH_3)_4CH_2^+]$ cations

Table 6. Atomic Coordinates and Isotropic Temperature Factors (Å^2) for **3**

Atom	x	y	z	B_{eq}[a]/Å^2
Ru	0.1342(1)	0.07748(8)	0.1880(1)	3.9
Fe	0.3785(2)	0.2008(1)	0.0091(3)	4.4
P	0.1379(4)	0.1139(3)	0.6829(6)	4.9
F(1)	0.147(1)	0.0557(8)	0.770(1)	9.8
F(2)	0.130(1)	0.1722(7)	0.596(1)	10.4
F(3)	0.074(1)	0.073(1)	0.631(2)	14.6
F(4)	0.206(1)	0.156(1)	0.728(2)	16.5
F(5)	0.197(1)	0.075(1)	0.612(2)	14.0
F(6)	0.084(2)	0.150(1)	0.751(2)	19.5
C(1)	0.291(1)	0.136(1)	0.061(2)	3.7
C(2)	0.366(2)	0.111(1)	0.090(2)	4.9
C(3)	0.409(1)	0.100(1)	−0.006(2)	6.8
C(4)	0.362(1)	0.115(1)	−0.085(1)	8.2
C(5)	0.290(1)	0.142(1)	−0.053(2)	5.5
C(6)	0.397(1)	0.287(1)	0.103(1)	17.6
C(7)	0.465(3)	0.256(2)	0.056(4)	15.3
C(8)	0.462(3)	0.269(2)	−0.040(5)	13.4
C(9)	0.395(3)	0.286(2)	−0.068(3)	10.8
C(10)	0.357(2)	0.302(1)	0.016(4)	11.5
C(11)	0.219(1)	0.152(1)	0.233(2)	5.2
C(12)	0.238(1)	0.085(1)	0.282(2)	4.1
C(13)	0.181(2)	0.065(1)	0.352(2)	8.5
C(14)	0.122(2)	0.121(1)	0.350(2)	9.4
C(15)	0.146(2)	0.172(1)	0.284(2)	7.0
C(16)	0.070(2)	0.072(1)	0.039(2)	7.4
C(17)	0.133(2)	0.022(2)	0.038(2)	6.6
C(18)	0.115(2)	−0.023(1)	0.121(3)	8.8
C(19)	0.048(2)	−0.006(2)	0.164(3)	10.4
C(20)	0.025(2)	0.054(2)	0.119(3)	10.4
C(21)	0.229(1)	0.162(1)	0.124(2)	4.4
H(21)	0.19(1)	0.20(1)	0.10(2)	6.9

a) $B_{eq} = 4/3(B_{11}a^2 + B_{22}b^2 + B_{33}c^2)$. B_{ij}'s are defined by $\exp[-(h^2B_{11} + k^2B_{22} + l^2B_{33} + 2klB_{23} + 2hlB_{13} + 2hkB_{12})]$.

Table 7. Selected Interatomic Distances for **3**

Atom 1–Atom 2	Dist./Å	Atom 1–Atom 2	Dist./Å
Ru(1)–Fe(1)	5.296(4)	Fe(1)–C(1)	2.05(2)
Fe(1)–C(2)	2.02(2)	Fe(1)–C(3)	2.01(2)
Fe(1)–C(4)	2.04(1)	Fe(1)–C(5)	2.04(2)
Fe(1)–C(6)	2.06(1)	Fe(1)–C(7)	1.91(3)
Fe(1)–C(8)	2.02(3)	Fe(1)–C(9)	1.93(4)
Fe(1)–C(10)	1.97(2)	Ru(1)–C(11)	2.10(2)
Ru(1)–C(12)	2.14(2)	Ru(1)–C(13)	2.22(2)
Ru(1)–C(14)	2.22(3)	Ru(1)–C(15)	2.18(2)
Ru(1)–C(16)	2.17(2)	Ru(1)–C(17)	2.16(2)
Ru(1)–C(18)	2.13(2)	Ru(1)–C(19)	2.20(3)
Ru(1)–C(20)	2.11(3)	Ru(1)–C(21)	2.43(2)
C(1)–C(2)	1.42(2)	C(1)–C(5)	1.43(2)
C(2)–C(3)	1.43(2)	C(3)–C(4)	1.31(2)
C(4)–C(5)	1.40(2)	C(6)–C(7)	1.44(4)
C(6)–C(10)	1.32(4)	C(7)–C(8)	1.24(4)
C(8)–C(9)	1.24(5)	C(9)–C(10)	1.29(5)
C(11)–C(12)	1.45(3)	C(11)–C(15)	1.44(3)
C(12)–C(13)	1.37(3)	C(13)–C(14)	1.47(4)
C(14)–C(15)	1.34(3)	C(16)–C(17)	1.44(4)
C(16)–C(20)	1.31(4)	C(17)–C(18)	1.39(4)
C(18)–C(19)	1.30(4)	C(19)–C(20)	1.35(4)
C(11)–C(21)	1.39(3)	C(1)–C(21)	1.53(2)
P–F(1)	1.57(1)	P–F(2)	1.57(1)
P–F(3)	1.49(2)	P–F(4)	1.53(2)
P–F(5)	1.54(2)	P–F(6)	1.44(2)

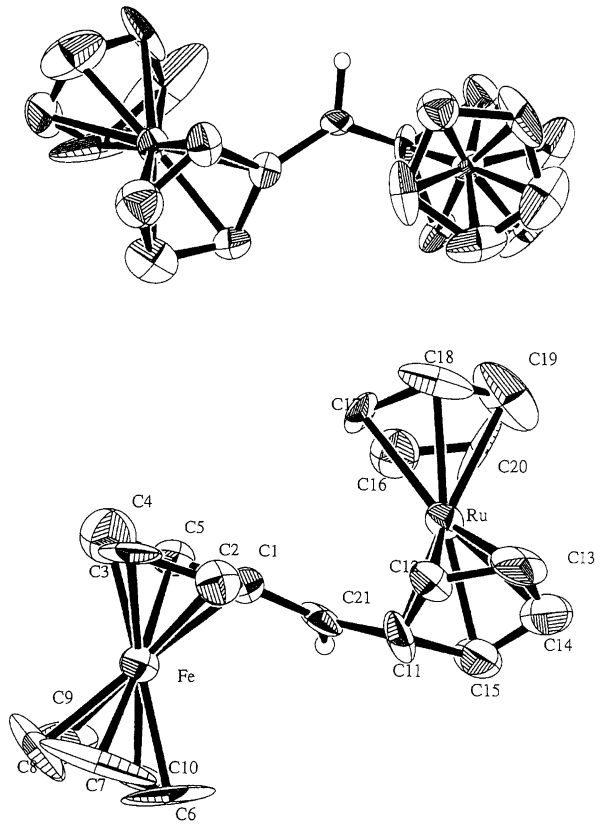

Fig. 5. ORTEP drawing of cation **3** showing the crystallographic numbering.

(M; Ru and Os, respectively), in which much more stable and shorter M–CH^+ bonds (2.270 and 2.244 Å, respectively) are found.[21—24] Thus, the flexibility conformation of cation **3** gives a shorter Ru–CH^+ bond, which causes the stability of the carbonium center cation.

The exocyclic C(11)–C(21) distance (1.39(3) Å) is much larger than the value of C(1)–C(21) (1.53(2) Å) and closer to the double-bond character (1.33 Å); also, the C(11)–C(12) (1.45(3) Å), C(11)–C(15) (1.44(3) Å) and C(13)–C(14) (1.47(4) Å) distances are somewhat larger than the values of C(12)–C(13) (1.37(3) Å) and C(14)–C(15) (1.34(3) Å), thus indicating the C(11—15) ring has a fulvene character. Thus, the cation is considered to be a resonance hybrid of the canonical structure **A** (α-carbonium) and **B** (fulvene), as shown in Scheme 2. However, the results of the present studies and several X-ray diffraction studies of analogous salts have revealed that the exocyclic methylene is greatly bent toward the central metal, so as to allow a direct interaction between the metal and empty of π^* orbital in the double bond ($C_1 = C^+$).[21—25] Moreover, the inclination structure of fulvene was verified by extended Hückel calculations.[26] Thus, the best representation of the cation may well be that shown in structure **B** for **3**.

As in the case of **2**, **3** gives clear ^1H and ^{13}C NMR peaks, as previously reported and NMR studies show that the structure of the cation in solution remains intact in a solid.[8] It is useful to discuss the δ_H values of **3** compared with those of **2** in line with structural points of view. The δ_H values of **3** are 4.36

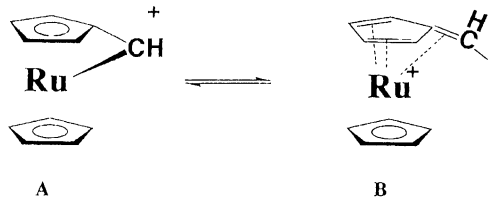

Scheme 2.

(5H), 4.72 (2H), and 4.84 (2H) for the Fc moiety; 5.02 (5H), 5.38 (2H), 5.95 (2H) for the Rc moiety; and $\delta = 7.65$ for the CH^+ proton in CD_3CN. The latter CH^+ signal shifts to a much lower field compared with the value of **2** ($\delta = 6.57$). This difference is caused by the Ru–CH^+ distance; i.e., the Ru–CH^+ distance (2.407(6) Å) of **2** is smaller than the value of **3** (2.43(1) Å). The higher positive CH^+ charge of **2** is fully neutralized, which produces a higher field shift of the CH^+ proton than that of **3**.

From the results obtained in the present studies, it can be concluded that [1.1]FcRc and $FcCH_2Rc$ react with [(RcH)-X]$^+PF_6^-$ (X : Cl, Br) giving α-carbonium hexafluorophosphate salts **1** and **3**, and that [1.1]FcRc reacts with [(RcH)-X]$^+BF_4^-$ giving an analogous tetrafluoroborate salt **2**. The most interesting difference between the structures of **1**—**3** is found in the Ru–C_α distance; i.e., the distances of **3** (2.43(2) Å) and **2** (2.407(6) Å) are significantly shorter than the value of **1** (2.51(1) Å). The main reason for the shorter Ru–C_α distance for **3** may be due to its flexibility conformation. The formation of Ru–C_α results in the stability of the higher positive CH^+ charge. Although cation **2** is not very flexibility, the presence the covalent Ru–CH^+ and hydrogen bond (BF_4^- and CH^+) gives stability to the α-carbonium cation. For both salts, the positive CH^+ charge spreads out to only the Rc moiety; thus, both give ferrocene-like ^{57}Fe-Mössbauer spectra over all temperatures.

On the other hand, due to the somewhat longer distance between the Ru and C_α, used to estimate the covalent Ru–C_α bond and absence of the hydrogen bond between the CH^+ and PF_6^- for **1**, the positive carbonium CH^+ charge is spread out over all of the Fc and Rc moieties. With increasing temperatures, the positive charge is increased in the Fc moiety because Fe is easily oxidized than Ru; therefore, temperature-dependent ^{57}Fe-Mössbauer spectra are found for **1**.

References

1) V. K. Kansal, W. E. Watts, and U. T. Mueller-Westerhoff, *Inorg. Chem.*, **23**, 2895 (1984).

2) A. Diaz, U. T. Mueller-Westerhoff, A. Nazzal, and M. Tanner, *J. Organomet. Chem.*, **236**, C45 (1982).

3) U. T. Mueller-Westerhoff, A. Nazzal, W. Prossdorf, J. J. Mayerle, and R. L. Collins, *Angew. Chem.*, **94**, 313 (1982).

4) U. T. Mueller-Westerhoff, T. J. Haas, G. F. Swiegers, and T. K. Leipert, *J. Organomet. Chem.*, **472**, 229 (1974).

5) U. T. Mueller-Westerhoff, *Angew. Chem., Int. Ed. Engl.*, **25**, 702 (1986); U. T. Mueller-Westerhoff, A. Nazzal W. Prossdorf, J. J. Mayerle, and R. L. Collins, *Angew. Chem., Int. Ed. Engl.*, **21**, 293 (1982); U. T. Mueller-Westerhoff, A. Nazzal, W. Prossdorf, J. J. Mayerle, and R. L. Collins, *Angew. Chem., Suppl.*, **1982**, 686.

6) U. T. Mueller-Westerhoff, A. L. Rheingold, and G. F. Swiegers, *Angew. Chem., Int. Ed. Engl.*, **31**, 1353 (1992).

7) M. Watanabe, I. Motoyama, and T. Takayama, *J. Organomet. Chem.*, in press.

8) M. Watanabe, T. Iwamoto, S. Nakashima, H. Sakai, I. Motoyama, and H. Sano, *J. Organomet. Chem.*, **448**, 167 (1993).

9) D. T. Cromer and J. T. Waber, "International Table for X-Ray Crystallography," The Kynoch Press, Birmingham, England (1974), Vol. IV, Table 2.2 A.

10) J. A. Ibers and W. C. Hamilton, *Acta Crystallogr.*, **17**, 781 (1964).

11) D. C. Creagh and W. J. McAuley, "International Table for X-Ray Crystallography," Kluwer Academic Publishers, Boston (1992), Vol. C, pp. 219—222, Table 4.2.6.8.

12) "TEXSAN: Crystal Structure Analysis Package," Molecular Structure Corporation (1985).

13) D. Bicker, B. Lukas, G. Neshvad, R. M. G. Roberts, and J. Silver, *J. Organomet. Chem.*, **263**, 225 (1984); R. A. Stukan, S. P. Gubin, A. N. Nesmeyanov, V. I. Goldanskii, and E. F. Makarov, *Teor. Eksp. Khim.*, **2**, 805 (1966).

14) R. Gleiter, R. Seeger, H. Binder, E. Fluck, and M. Cais, *Angew. Chem., Int. Ed. Engl.*, **11**, 1028 (1972).

15) A. L. Rheingold, U. T. Mueller-Westerhoff, G. F. Swiegers, and T. J. Haas, *Organometallics*, **11**, 3411 (1992).

16) N. J. Mammano, A. Zalkin, A. Landers, and A. L. Reingold, *Inorg. Chem.*, **16**, 297 (1977).

17) P. Seiler and J. D. Dunitz, *Acta Crystallogr., Sect. B*, **35B**, 1068 (1979).

18) L. Pauling, "The Nature of Chemical Bond," Cornell Univ. Press, (1960).

19) V. G. Andrianov, B. P. Biryukov, and Y. T. Struchkov, *Zh. Strukt. Khim.*, **10**, 1129 (1969).

20) S. Lupan, M. Kapon, M. Cais, and F. H. Herbstein, *Angew. Chem., Int. Ed. Engl.*, **11**, 1025 (1972).

21) M. I. Rybinskaya, A. Z. Kreindlin, and S. S. Fadeeva, *J. Organomet. Chem.*, **358**, 363 (1988).

22) M. I. Rybinskaya, A. Z. Kreindlin, Y. T. Struchkov, and A. I. Yanovsky, *J. Organomet. Chem.*, **359**, 233 (1989).

23) A. I. Yanovsky, Y. T. Struchkov, A. Z. Kreindlin, and M. I. Rybinskaya, *J. Organomet. Chem.*, **369**, 125 (1989).

24) U. Turpeinen, A. Z. Kreindlin, P. V. Petrovskii, and M. I. Rybinskaya, *J. Organomet. Chem.*, **441**, 109 (1992).

25) L. E. Schock, C. P. Brock, and T. J. Marks, *Organometallics*, **6**, 232 (1987)

26) R. Gleiter and R. Seeger, *Helv. Chim. Acta*, **54**, 1217 (1971).